

## AN ANALYSIS OF SOME FACTORS INFLUENCING THE TOUGHNESS OF POROUS SINTERED MATERIALS

J. R. Moon, A. Molinari

### **Abstract**

*The toughness of materials can be measured in a number of ways, but all are measures of how much of the energy supplied by a load is required to bring about fracture. In PM materials it is most often interpreted in terms of the fraction of the cross-sectional area available to support a load. A question arises about where in the material the energy supplied by the applied load is absorbed. This paper describes an attempt to calculate one measure of toughness by analysing the elastic energy expended in the material as a whole and the plastic deformation energy expended in the regions adjacent to sinter necks. Although, of necessity, greatly simplified, it demonstrates the relative significance of the elastic and plastic contributions to toughness in relation to (a) the relative density of the material, (b) the yield and fracture strengths of the matrix material and (c) the ductility of the matrix material.*

**Keywords:** *PM materials, toughness, relative density, elastic and plastic strain energy*

### INTRODUCTION

In interpreting the toughness of sintered PM materials much emphasis is placed on the fraction of the cross-sectional area available to support a load [1-3]. But the work done in elastically deforming the material as a whole and in plastically deforming the volumes that extend from the plane of a sinter neck into the adjacent particles has received comparatively little attention. Intuitively, we would expect that the greater is the deformed volume, the greater will be the toughness. Previous considerations based on these thoughts suggest that the volumes capable of plastic deformation are determined by the yield and fracture stresses of the matrix material [4]. An attempt is made here to calculate toughnesses relative to those of fully dense materials, based on analyses of [i] the elastic deformation of the material as a whole and [ii] the plastic deformation of the smaller volumes close to inter-particle necks and their work hardening characteristics.

Before looking at the matter in more detail, it is worth considering the nature of the stresses and strains experienced by sinter necks, as illustrated in Fig.1. The strains resolve into tension and shear components, which, of course, vary from the centre of a neck to its surface. To take such complexity into account would be overwhelming and so the following calculations are based in a simplified model of a sinter neck under uniform tension only.

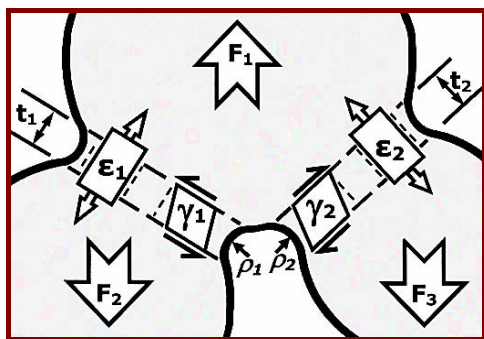


Fig.1. Illustrating the loading and the tension and shear components of strains experienced by sinter necks. For mechanical equilibrium, all forces and moments must add vectorially to zero.

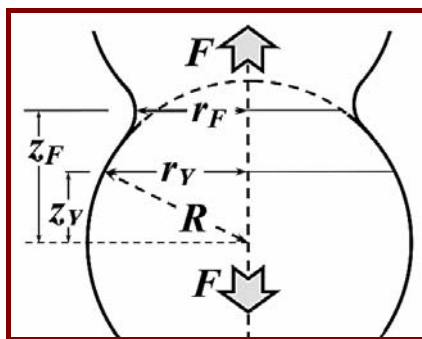


Fig.2. A single sinter neck between two spherical particles of identical sizes, subject to a uniaxial tension load of  $F$ .

## RESULTS AND DISCUSSION

### The volume deformed plastically

Localised plastic deformation in the region of sinter necks

At fracture the local stress in a sinter neck under tension is the fracture stress of the matrix material,  $\sigma_F$ . The whole volume deforms elastically by differing amounts depending on the local stress. A smaller volume extending into the particles from the neck deforms plastically, the limit being at the plane where the local stress reduces to the yield stress of the matrix material,  $\sigma_Y$ . The volume plastically deformed in one particle is taken to be the same as the volume of the spherical cap cut off by the yield-plane; some of this material has been transferred into the sinter neck, but all the material originally in the cap has been plastically deformed.

This volume is;

$$V_{plastic} = \left[ \frac{2}{3}R^3 - \left( R^2z_Y - \frac{1}{3}z_Y^3 \right) \right] \tag{1}$$

where,

$$z_Y^2 = R^2 - r_Y^2 \quad \text{and} \quad \left( \frac{r_Y}{R} \right)^2 = \frac{\sigma_R}{\sigma_Y} \quad \text{and} \quad \left( \frac{r_F}{R} \right)^2 = \frac{\sigma_R}{\sigma_F}$$

and  $\sigma_R$  is the local stress at the plane through the centre of the particle. Re-arranging in terms of stresses, gives;

$$V_{plastic} = \frac{2\pi R^3}{3} - \frac{\pi R^3}{3} \left( 2 + \frac{\sigma_R}{\sigma_Y} \right) \sqrt{1 - \frac{\sigma_R}{\sigma_Y}} \quad \text{and} \quad \frac{\sigma_R}{\sigma_Y} = \frac{\sigma_F}{\sigma_Y} \frac{\sigma_R}{\sigma_F} \left( \frac{r_F}{R} \right)^2 \tag{2a}$$

or, as a fraction of the whole particle;

$$\frac{V_{plastic}}{V_{particle}} = \frac{1}{2} - \frac{1}{4} \left( 2 + \frac{\sigma_F}{\sigma_Y} \left( \frac{r_F}{R} \right)^2 \right) \sqrt{1 - \frac{\sigma_F}{\sigma_Y} \left( \frac{r_F}{R} \right)^2} \tag{2b}$$

The analysis can be extended to consider the material as a whole. Each particle is in contact with several others. Although the local stress system will differ from neck to

neck as in Fig.1, we simplify by assuming that each sinter neck makes the same contribution, the total volume within one particle that is deformed plastically is given by equation 2b multiplied by the co-ordination number. For the material as a whole, we have

$$\frac{V_{plastic}}{V_{material}} = \frac{V_{plastic}}{V_{particle}} N_C \rho_r \tag{3}$$

Where  $N_C$  is the co-ordination number representative of the particle packing and  $\rho_r$  is the relative density of the material. For spheres in the so-called random close packed arrangement,  $N_C$  is generally thought to be about 6 [5,6]. Remembering that in the case of a PM part, the particles have been pushed together during compaction, a rather higher coordination number is used here; 8 was chosen.

Density and neck size are not independent quantities. The random close packed condition has a relative density of close to 0.644 [7,8]. To estimate when full density is attained, consider four overlapping spheres, centred at the corners of a tetrahedron (Fig.3) and of a size to meet at the centre of the tetrahedron - that is to reduce the pore size to zero.

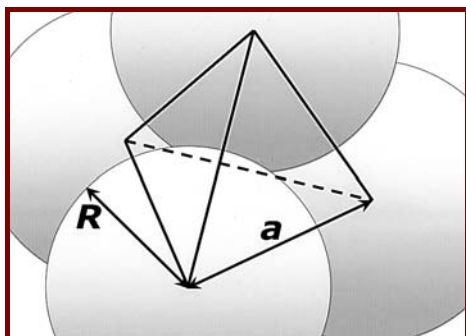


Fig.3. The geometry of overlapping spheres centred at the corners of a tetrahedron.

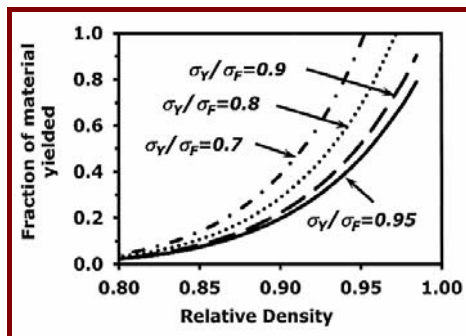


Fig.4. Calculated fraction of the whole PM material that has yielded as functions of relative density and the ratio of true yield to true fracture stress of the solid material.

Geometry gives the relative size of the contact plane when  $\rho_r=1$ ;  $r/R = 0.774$ .

From these observations, we have;

$$\rho_r = 0.644 + 0.45r/R \tag{4}$$

Putting all this together allows calculation of the fraction of the overall material that has yielded as functions of the relative density and of the ratio of yield to fracture strength of the solid material that has been deformed Fig.4 illustrates.

### What do we mean by toughness?

Figure 5 gives examples of stress/strain curves for a few, model, fully dense materials in uniaxial tension.  $W/V$  is the work done on the material per unit volume, the strain energy density, until it fractures. Note that material D requires the most work to be done to bring it to fracture and that material C illustrates the importance of ductility.

Figure 6 shows the relationship established by experiment between the strain energy density to fracture in tension and the un-notched impact energy for the same PM steels. It justifies the adoption of  $W/V$  as an indicator of toughness, even though the loading conditions are very different.

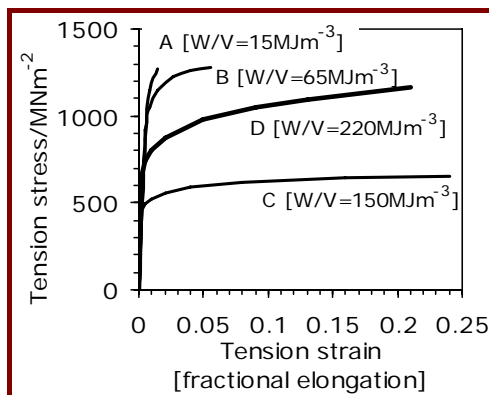


Fig.5. Examples of true-strain / true-stress curves for model, fully dense materials.

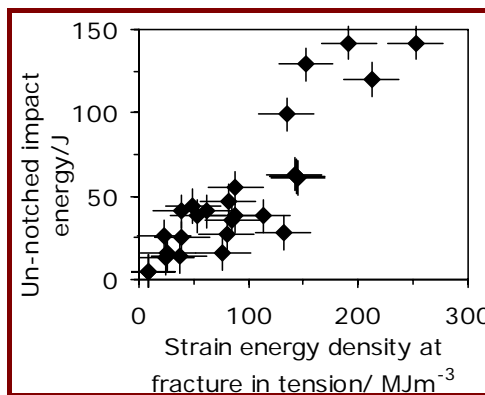


Fig.6. Calculated fraction of the whole PM material that has yielded as functions of relative density and the ratio of true yield to true fracture stress of the solid material.

### Stresses and Work

#### Plastic

The work done to plastically deform the material from yielding to an arbitrary strain,  $\epsilon^*$ , when subject to a uniaxial tension load is:

$$\frac{W}{V} = \int_{\epsilon_y}^{\epsilon^*} \sigma d\epsilon \tag{5}$$

with  $\sigma$  &  $\epsilon$  being the true stress and true-strain, respectively.

Many expressions exist to describe the plastic flow of materials. For simplicity, we choose a linear work hardening model.

$$\sigma^* = \sigma_Y + n\epsilon^* \tag{6a}$$

and note that

$$n = (\sigma_F - \sigma_Y) / \epsilon_F \tag{6b}$$

and

$$\left(\frac{W}{V}\right)_{plastic} = \frac{1}{2} \epsilon^* (\sigma^* - \sigma_Y) = \frac{1}{2} \frac{(\sigma^* - \sigma_Y)^2}{(\sigma_F - \sigma_Y)} \epsilon_F \tag{7}$$

$\sigma^*$  varies inside the yielded volume from  $\sigma_F$  at the sinter neck (where fracture occurs) to  $\sigma_Y$  at the boundary between yielded and un-yielded volumes. The easiest approach is to use the average stress in the yielded region for  $\sigma^*$ .

$$\sigma_{AV} = \frac{F}{\pi r_{AV}^2} \quad \text{and} \quad \sigma_{AV} = \frac{F}{\pi} \frac{1}{(r_F - r_Y)} \int_{r_Y}^{r_F} \frac{dr}{r^2} \tag{8a}$$

which yields

$$\sigma^* \approx \sigma_{AV} = \sqrt{\sigma_F \sigma_Y} = \sigma_F \sqrt{\frac{\sigma_Y}{\sigma_F}} \tag{8b}$$

In these expressions,  $\sigma_Y$  and  $\sigma_F$  refer to the properties of the metal making up the particle and the sinter neck, which are assumed to be homogeneous and identical. Table 1

gives data for a commonly used, fully solid, heat-treatable low-alloy steel; for purposes of calculation here,  $\sigma_F$  is taken to be 2000MPa. For true-strains to fracture, calculations are based on the measured reductions in cross-sectional area at fracture (% elongation is a useful measure for comparative purposes, but, in this context is meaningless, being as much a function of test-piece geometry as of material; reduction in area to fracture avoids this complication)

Tab.1. Wrought 4340: 0.4C-0.8Cr-1.8Ni-0.25Mo (0.75Mn-0.3Si). Oil quenched from 845°C.

Tempering temperature [°C]	Yield [MPa]	UTS [MPa]	Yield/UTS	% elong	% RA
205	1860	1980	0.94	11	39
315	1620	1760	0.92	12	44
425	1365	1500	0.91	14	48
540	1160	1240	0.94	17	53
650	860	1020	0.84	20	60
705	740	860	0.86	23	63

**Elastic resilience**

The work done per unit volume to deform a solid material elastically to a stress of  $\sigma$  is

$$\left(\frac{W}{V}\right)_{elastic} = \int_0^\epsilon \sigma d\epsilon = \int_0^\sigma \sigma(d\sigma/E) = \sigma^2/2E \tag{9}$$

In this case, the whole particle is deformed. As before, we use the average stress in the whole particle.

$$\sigma_{AV} = \sqrt{\sigma_F \sigma_R} = \sigma_F \sqrt{\frac{\sigma_R}{\sigma_F}} \tag{10}$$

Where  $\sigma_R$  is the stress acting at the full diameter of the particle and  $\sigma_R = \sigma_F (r_F/R)^2$ , where  $R$  is the radius of the particle

which gives us,  $\sigma_{AV} = \sigma_F (r_F/R)$  and, for the whole particle

$$\left(\frac{W}{V}\right)_{elastic} = \frac{\sigma_F^2}{2E} \left(\frac{r_F}{R}\right)^2 \tag{11a}$$

and for the material as a whole

$$\left(\frac{W}{V}\right)_{elastic} = \rho_r \frac{\sigma_F^2}{2E} \left(\frac{r_F}{R}\right)^2 \tag{11b}$$

Figures 7 shows the separate contributions to toughness from the plastic and elastic deformations.

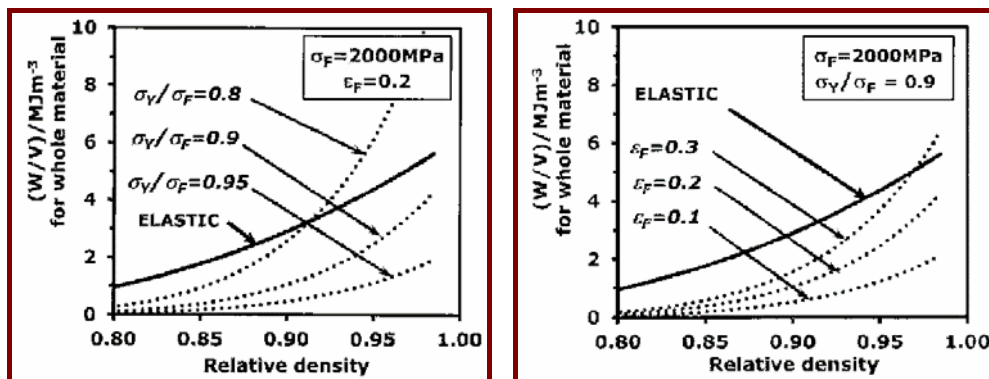


Fig.7a,b. The plastic & elastic strain energy densities to fracture for a porous material as functions of the relative density and (a) the ratio of true yield stress to true fracture stress; (b) the ductility of the solid material (as measured by reduction in cross-sectional area at fracture).

Not unexpectedly, the lower is the ratio  $\sigma_Y/\sigma_F$  and the more ductile is the matrix material then the tougher is the overall material. The elastic component dominates when the density is low and when  $\sigma_Y/\sigma_F$  is higher. This reflects the relative sizes of the volumes deformed; plastic deformation is confined to a fraction of a particle which depends on both the size of the sinter neck and the properties of the material [ $\sigma_Y/\sigma_F$ ]; elastic deformation involves the whole particle, although, of course, it experiences a range of stresses.

The analysis can be extended by reference to the relative load bearing area,  $\Phi$ , as identified by Molinari et al [1]. Their experimental measurements of the relationship between this quantity and the relative density is illustrated in Fig.8, adapted from their paper; note that this relationship holds only in the regime of interconnected pores.

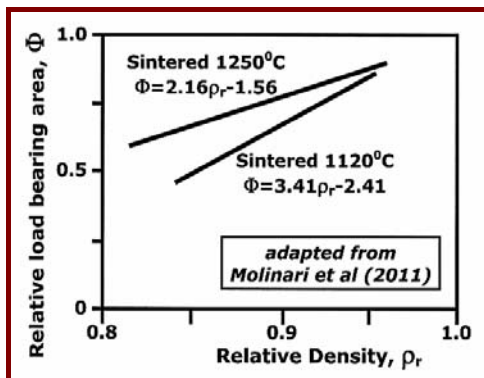


Fig.8. The relative load bearing area,  $\Phi$ , as a function of relative density [adapted from Molinari et al (1)].

The outcome is in Fig.9, which shows the calculated total toughness (elastic + plastic) as functions of relative density and of  $\Phi$ . Comparison of Fig.9a and 9b demonstrates that the two approaches to the interpretation of toughness are compatible with one another.

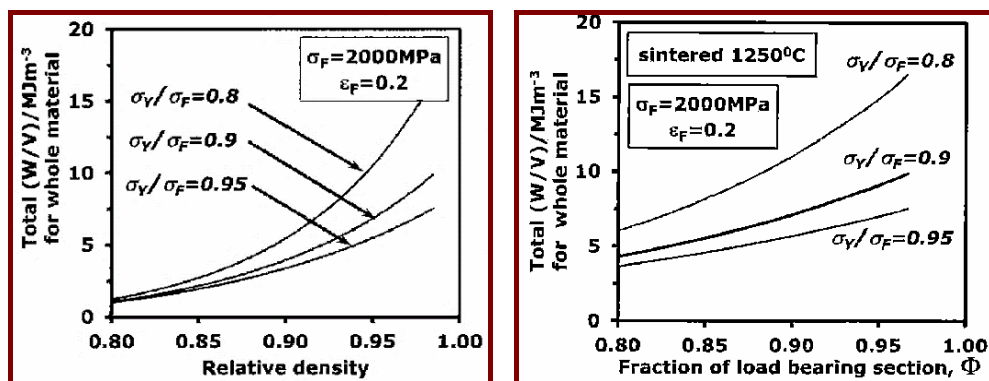


Fig.9a,b. The calculated toughness of a porous material as functions of (a) the relative density,  $\rho_r$ ; (b) the fraction of load bearing area,  $\Phi$ .

For comparison, Fig.10, taken and adapted from Molinari et al [1], shows toughnesses measured by impact tests as functions of microstructural component, relative load bearing area and relative density.

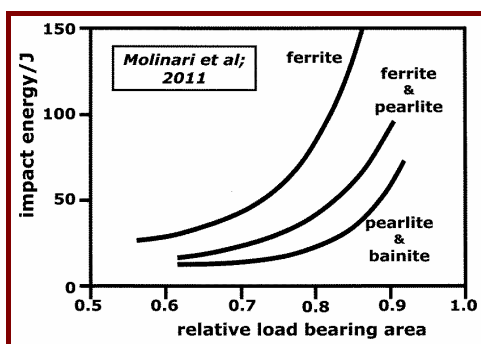


Fig.10. Impact energies of PM steels, illustrating the influences of microstructural component and of the relative load bearing area [1].

## CONCLUSIONS

It has to be accepted that the analysis is capable of improvement. In particular, the model is oversimplified, as is the method of assessing both the plastic and elastic strain energy densities from an average stress in the appropriate region. To carry out a more complete analysis would involve introducing too many adjustable variables to describe plastic flow and involve some awkward integrations that have been avoided here.

Nevertheless, the analysis provides an acceptable interpretation of many experimental observations. In particular, it shows, for a given fracture stress at a sinter neck, the relative significance of the continuity of the porous material (sinter-neck sizes/particle size) and of the properties that define the plasticity of the solid material (yield-stress/fracture stress and ductility). The elastic contribution dominates when sinter neck sizes are small, when  $\sigma_Y/\sigma_F$  of the matrix material is high and when the matrix ductility is low. It becomes progressively less dominant when  $\sigma_Y/\sigma_F$  is smaller, the sinter neck size increases and the ductility of the matrix increases.

## REFERENCES

- [1] Molinari, A., Menapace, C., Santuliana, E., Straffelini, G.: Powder Metallurgy Progress, vol. 11, 2011, p. 12
- [2] Vedula, KM., Heckel, RW.: Modern Developments in Powder Metallurgy, vol. 12, 1981, p. 759
- [3] Dudrová, E., Kabátová, M.: Powder Metallurgy Progress, vol. 8, 2008, p. 59
- [4] Moon, JR. In: Deformation and fracture in structural PM materials. High Tatras, Slovakia. Košice : Slovak Academy of Sciences, 2005, p. 138
- [5] Bernal, JD., Mason, J.: Nature, vol. 188, 1960, p. 910
- [6] Rintoul, MD., Torquato, S.: Physical Review E, vol. 58, 1998, p. 532
- [7] Scott, GD., Kilgour, DM.: Journal of Physics D: Applied Physics, vol. 2, 1969, p. 863
- [8] Esen, Z., Tarhan Bor, E., Bor, S.: Turkish J Eng Env Sci, vol. 33, 2009, p. 207